Probing the Environment of Tubulin-Bound Paclitaxel Using Fluorescent Paclitaxel Analogues†

Suparna Sengupta,‡ Thomas C. Boge,§ Yanbin Liu,§ Michael Hepperle,§ Gunda I. Georg,§ and Richard H. Himes*,‡

Departments of Biochemistry and Medicinal Chemistry, University of Kansas, Lawrence, Kansas 66045

Received November 22, 1996; Revised Manuscript Received February 26, 1997⊗

ABSTRACT: To determine the environment of different positions in the paclitaxel molecule when bound to tubulin, we have synthesized six fluorescent analogues in which a (dimethylamino)benzoyl group has been introduced into the 7- and 10-positions, and the benzoyl groups at the 2- and *N*- as well as the 3′-phenyl ring have been modified with dimethylamino functions. In a tubulin assembly assay, the *N*-*m*- and *N*-*p*-(dimethylamino)benzoyl derivatives had activities comparable to the activity of paclitaxel. The 2-, 3′-, and 10-analogues had slightly reduced activity, and the 7-derivative was about 5% as active as paclitaxel. On the basis of the results of studies of the effect of solvents on the fluorescence emission spectra, it is proposed that the unbound analogues form hydrogen bonds with protic solvents. But the 7- and 10-substituted analogues appear to be more affected by protic solvents than the other analogues. Previously, we studied the binding of the *N*-*meta* derivative to tubulin and microtubules [Sengupta, S., et al. (1995) *Biochemistry 34*, 11889−11894]. In this study, we extended the studies to include the 2-, 7-, and 10-derivatives. Similar to the *N*-substituted analogue, binding of the 2-derivative to tubulin was accompanied by a large blue shift, whereas a very small shift occurred when the 7- and 10-substituted derivatives bound. The 2- and *N*-substituted analogues bind to microtubules with an increase in fluorescence intensity over that which was observed with tubulin, whereas binding of the 7- and 10-substituted analogues was accompanied by a large quenching in fluorescence. This quenching may be due to the presence of charged residues in the protein near the 7- and 10-(dimethylamino)benzoyl groups or to π stacking of the groups with an aromatic side chain. The presence of paclitaxel with microtubules prevented the fluorescence increase of the 2- and *N*-derivatives and quenching of the 7- and 10-derivatives. The difference in behavior of the fluorescent analogues upon binding to polymerized tubulin, coupled with the solvent studies on the free drugs, suggests that the 2- and *N*-benzoyl groups of paclitaxel bind in a hydrophobic pocket of tubulin but could participate in hydrogen bonding, and the 7- and 10-positions are in a more hydrophilic environment.

Antimitotic agents fall into two classes, one whose members inhibit tubulin self-assembly and depolymerize microtubules and another whose members stabilize microtubules and promote microtubule formation from tubulin. Paclitaxel, as well as epothilone A and B (Bollag et al., 1995), and discodermolide (ter Haar et al., 1996) fall into the second class. At low concentrations, paclitaxel suppresses microtubule dynamics *in vitro* (Derry et al., 1995). Such low concentrations also stabilize cellular mitotic spindle microtubules by inhibiting microtubule instability (Jordan et al., 1993; Yvon et al., 1996), leading to apoptosis (Jordan et al., 1996). At high concentrations, the drug upsets the tubulin−microtubule equilibrium by inducing microtubule formation and bundling *in vitro* (Schiff & Horwitz, 1980) and in cells (Jordan et al., 1993). Whether the suppression of microtubule dynamics or disturbance of the tubulin−microtubule equilibrium is more clinically important is not known at this time.

Many analogues of paclitaxel have been synthesized in recent years in the hope of finding more effective derivatives, and for use in determining the binding environment and binding site of the drug in tubulin. It is known that paclitaxel can tolerate a large number of modifications at most positions around the molecule without drastically affecting its biological activity [for reviews, see Hepperle and Georg (1994) and Georg et al. (1995b,c)]. Because fluorescent analogues of a drug can provide useful information about the environment of the bound form of the drug, and the mechanism of drug binding, we and others have been engaged in the synthesis of fluorescent paclitaxel analogues (Sengupta et al., 1995; Souto et al., 1995; Han et al., 1996). Previously, we showed that *N*-debenzoyl-*N*-[3-(dimethylamino)benzoyl]paclitaxel (N-*m*DMAT[1]) has a biological activity similar to that of paclitaxel and that its binding to both polymeric and dimeric tubulin is accompanied by a large change in its fluorescent

† This work was supported by National Institutes of Health Grant CA 55141. T.C.B. was supported by a postdoctoral fellowship from the Hoechst Marion Roussel Scientific Education Partnership. S.S., Y.L., and M.H. were recipients of Kansas Health Foundation, Wichita, Kansas, Cancer Scholar Grants.

* Author to whom correspondence should be addressed: Richard H. Himes, Department of Biochemistry, University of Kansas, Lawrence, KS 66045. Phone: (913) 864-3813. Fax: (913) 864-5321. E-mail: himes@kuhub.cc.ukans.edu.

‡ Department of Biochemistry.

§ Department of Medicinal Chemistry.

⊗ Abstract published in *Advance ACS Abstracts,* April 1, 1997.

[1] Abbreviations: N-*m*DMAT, *N*-debenzoyl-*N*-[*m*-(dimethylamino)-benzoyl]paclitaxel; N-*p*DMAT, *N*-debenzoyl-*N*-[*p*-(dimethylamino)-benzoyl]paclitaxel; 2-*m*DMAT, 2-debenzoyl-2-[*m*-(dimethylamino)-benzoyl]paclitaxel; 3′-*m*DMAT, 3′-dephenyl-3′-[*m*-(dimethylamino)-phenyl]paclitaxel; 10-*m*DMAT, 10-deacetyl-10-[*m*-(dimethylamino)-benzoyl]paclitaxel; 7-*m*DMAT, 7-dehydroxy-7-[*m*-(dimethylamino)-benzoyl]oxy]paclitaxel; EDC, 1-ethyl-3-[3-(dimethylamino)propyl]-carbodiimide; DCC, 1,3-dicyclohexylcarbodiimide.

S0006-2960(96)02891-7 CCC: $14.00

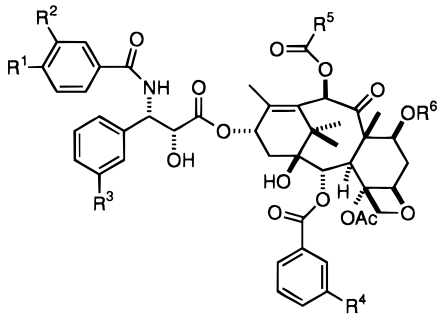

Paclitaxel	R^1=R^2=R^3=R^4=R^6=H, R^5=Me
N-*m*DMAT	R^1=R^3=R^4=R^6=H, R^2=NMe_2, R^5=Me
N-*p*DMAT	R^1=NMe_2, R^2=R^3=R^4=R^6=H, R^5=Me
2-*m*DMAT	R^1=R^2=R^3=R^6=H, R^4=NMe_2, R^5=Me
7-*m*DMAT	R^1=R^2=R^3=R^4=H, R^5=Me, R^6=*m*-N,N-dimethylbenzoyl
3′-*m*DMAT	R^1=R^2= R^4=R^6=H, R^3=NMe_2, R^5=Me
10-*m*DMAT	R^1=R^2=R^3=R^4=R^6=H, R^5=*m*-N,N-dimethylphenyl

FIGURE 1: Structures of paclitaxel and fluorescent paclitaxel analogues.

properties (Sengupta et al., 1995). In this study, we have introduced the fluorophore into different positions around the paclitaxel molecule by preparing five (dimethylamino)-benzoyl and one (dimethylamino)phenyl-substituted analogues (Figure 1) and have compared their fluorescent properties in the free and tubulin-bound forms. The analogues with substitutions at the *N*-benzoyl and 2-benzoyl positions behave similarly in their interaction with microtubules, leading to a blue shift and an enhancement in fluorescence intensity, whereas the fluorescence of the 7- and 10-substituted analogues is quenched upon binding to microtubules. When bound to unpolymerized tubulin or to the tubulin−podophyllotoxin complex, the fluorescence of all four derivatives undergoes a blue shift as well as an enhancement.

EXPERIMENTAL PROCEDURES

Materials. Microtubule protein was prepared from bovine brain by three cycles of an assembly−disassembly procedure (Tiwari & Suprenant, 1993). Pure tubulin was prepared from this preparation using phosphocellulose−Biogel P-10 chromatography (Algaier & Himes, 1988) and was stored at −80 °C after drop-freezing in liquid nitrogen. Before use, the tubulin was thawed and any aggregated protein was removed by centrifugation at 27000*g* for 10 min. Paclitaxel was purchased from Hauser Chemical Research, Inc. (Boulder, CO). [^{3}H]Paclitaxel was purchased from Moravek Biochemicals. Podophyllotoxin was obtained from ICN Chemical Co.

Polymerization Assays. Tubulin polymerization was induced by paclitaxel or the substituted analogues in PEM buffer [0.1 M Pipes (pH 6.9), 1 mM $MgSO_4$, and 1 mM EGTA]. Two methods were used to follow the assembly process and measure the effectiveness of paclitaxel and its analogues in inducing microtubule assembly. In one, the turbidity at 350 nm was measured at 37 °C in a thermostated Shimadzu UV 2100U spectrophotometer. The other, a centrifugation assay (Sengupta et al., 1995), was used to determine the EC_{50} values, the concentration of the drug causing assembly of 50% of the initial protein concentration. The protein concentration was measured by the Bradford procedure (Bradford, 1976).

Competition of [^{3}H]Paclitaxel Binding to Tubulin. A solution of 5 μM [^{3}H]paclitaxel and 5 μM tubulin was incubated in PEM buffer and 0.5 mM GTP at 37 °C in a 0.5 mL volume with various concentrations of the analogues. After 15 min, the mixture was centrifuged in a TL-100 Beckman ultracentrifuge for 5 min at 40000*g*. Warm PEM buffer was added to the pellet without stirring and then removed. The pellet was dissolved in 0.1 M NaOH. Aliquots from the solution were used to measure bound [^{3}H]paclitaxel and the protein concentration.

Fluorescence Measurements. A Perkin-Elmer MPF-44B spectrofluorometer attached to a circulating temperature-controlled bath was used to record all fluorescence spectra. Both excitation and emission band-passes were 5 nm, and all fluorescence values reported were uncorrected. Blank values for the solvents were subtracted from the fluorescence spectra of the analogues.

Electron Microscopy. Assembled tubulin samples were fixed with 0.25% glutaraldehyde and diluted when necessary. Following adherence for 45 s to grids coated with Formvar and carbon and rinsing with water, they were negatively stained with 2% uranyl acetate and examined in a JEOL JEM-1200 Ex II microscope.

Synthesis of the Analogues. The six paclitaxel fluorescent probes were synthesized according to procedures developed in our laboratory using paclitaxel or baccatin III as the starting materials (Georg et al., 1995c). N-*m*DMAT and N-*p*DMAT were prepared from *N*-debenzoylpaclitaxel by acylation with *m*- and *p*-(dimethylamino)benzoyl chloride under Schotten-Baumann conditions (Georg et al., 1994). 2-*m*DMAT was obtained from a 2-debenzoylpaclitaxel derivative by acylation (DCC coupling) with *m*-(dimethylamino)benzoic acid (Georg et al., 1995a). Reaction of 2′-protected paclitaxel with *m*-(dimethylamino)benzoic acid, catalyzed by EDC, provided, after deprotection of the 2′-silyl group, 7-*m*DMAT (Georg et al., 1996b). The 3′-*m*DMAT derivative was prepared from baccatin III, using an *N*-benzoyl-β-lactam [(3*R*,4*S*)-1-benzoyl-3-[(*tert*-butyldimethylsilyl)oxy]-4-[3-(dimethylamino)phenyl]-2-azetidinone] as the precursor for the C13 side chain of the analogue (Georg et al., 1996a). Removal of the C10 acetyl group of 2′-7-chloroacetyl-protected paclitaxel (Datta et al., 1995; Zheng et al., 1995) was followed by protection of the hydroxyl groups at 2′ and 7 as chloroacetates (Rao et al., 1995). Reacylation at C10 with *m*-(dimethylamino)benzoic acid (EDC) and removal of the protecting groups gave 10-*m*DMAT. A complete description of the syntheses is available in the Supporting Information.

The purity of the compounds was verified by HPLC analysis on a C-18 reverse phase column using 70% methanol or 50% acetonitrile as the solvent.

Molecular Modeling. Structures were built using the "Sketch Molecule" function of the molecular modeling software package SYBYL, utilizing the conformation of paclitaxel in aqueous solution (hydrophobic collapse) as a template (Vander Velde et al., 1993). Each structure was then subjected to an energy minimization using the standard Tipos force field.

RESULTS

Synthesis and Assembly-Promoting Properties. Yields of the products ranged from 46 to 70%. ^{1}H-NMR and mass

Table 1: EC_{50} Values and Spectra Maxima of the Paclitaxel Analogues

compound	EC_{50} (μM)	absorption maxima (nm)[a]	emission maxima (nm)[a]
paclitaxel	0.8	227, 273	
N-*m*DMAT	1.0	228, 263, 330	455
N-*p*DMAT	1.1	230, 305	363
2-*m*DMAT	2.7	230, 263, 345	473
7-*m*DMAT	18	230, 263, 341	465
10-*m*DMAT	2.7	230, 263, 344	472
3′-*m*DMAT	4.5	230, 260, 306	357

[a] Spectra were recorded in MeOH and are uncorrected. The absorption maxima in PEM buffer were essentially the same as in methanol.

spectra were consistent with the structures. HPLC analysis showed the compounds to be at least 98% pure. To test their effectiveness in inducing microtubule assembly, the analogues were compared to paclitaxel using a centrifugation assay. The EC_{50} values are shown in Table 1. Both N-DMAT derivatives are similar in activity to paclitaxel, and the 2-, 3′-, and 10-derivatives are slightly less active. Substitution at the 7-position caused the largest decrease in activity. In all cases, electron microscopy was used to verify the formation of microtubules.

Spectral Properties of the Analogues. The absorption and fluorescence emission maxima of the six paclitaxel analogues in methanol are presented in Table 1. The spectra of N-*m*DMAT, 2-*m*DMAT, 7-*m*DMAT, and 10-*m*DMAT are similar as might be expected because they all contain a dimethylamino substituent in the *meta* position of a benzoyl group; however, N-*p*DMAT has the substituent in the *para* position of the benzoyl group, and 3′-*m*DMAT contains a *m*-(dimethylamino)phenyl group.

Studies of the effects of different solvents on the fluorescence emission spectrum of a fluorophore can provide information about the environment of the fluorophore and by analogy the nature of the binding environment in a macromolecule. Interpretation of these changes requires consideration of both general and specific solvent effects. We examined the spectra of the six analogues in solvents of different polarity, some protic and some nonprotic (Table 2). The six derivatives showed a blue shift when the spectra were taken in acetonitrile and cyclohexane as compared to water, as is expected for a general solvent effect. However, in the protic solvents methanol and 2-propanol, the shifts cannot be attributed to polarity alone. In methanol, the spectra are red shifted compared to those in acetonitrile even though the polarity of methanol is less than that of acetonitrile and the extent of the shift in 2-propanol compared to acetonitrile does not reflect the large difference in dielectric constants between these two solvents. Differences also exist among the compounds. In the case of the 7- and 10-derivatives, there is a red shift in methanol compared to water, whereas with all the other compounds, blue shifts were obtained. The large effect of the protic solvents is observed when the spectra were taken in cyclohexane containing 3% ethanol, in which the emission maxima underwent large red shifts compared to those in cyclohexane alone. Increasing the ethanol concentration to 10% had no further effect. As shown in Table 2, the emission maxima of the analogues when bound to tubulin, to be discussed later, are very close to those in the cyclohexane/ethanol mixture. Further studies with N-*p*DMAT and 3′-*m*DMAT were not performed as the excitation bands for these compounds overlap with the tryptophan excitation band of the protein.

Competition of Paclitaxel Binding to Tubulin. We previously studied the binding of N-*m*DMAT to the paclitaxel binding site of tubulin (Sengupta et al., 1995). To ensure that 2-*m*DMAT, 7-*m*DMAT, and 10-*m*DMAT also bind to tubulin at the same site as paclitaxel, a competition study using [^{3}H]paclitaxel was performed. Using 5 μM tubulin, 5 μM [^{3}H]paclitaxel, and various concentrations of the analogues, we found 35, 14, and 44% inhibition of binding to microtubules by 30 μM 2-*m*DMAT, 7-*m*DMAT, and 10-*m*DMAT, respectively. These values are consistent with the EC_{50} values which show a weaker capacity of these compounds compared to paclitaxel to induce microtubule assembly, with 7-*m*DMAT being the weakest. Because of solubility limitations, concentrations of the drugs higher than 30 μM could not be used.

Changes in Drug Fluorescence upon Binding to Tubulin. Upon the addition of tubulin to the 2-, 7-, or 10-derivatives, the fluorescence intensity of the drugs increased instantaneously, similar to what happens in the case of the *N*-derivative (Sengupta et al., 1995). In the case of 2-*m*DMAT (Figure 2A), the increase was 8-fold, whereas for 7- (data not shown) and 10-*m*DMAT (Figure 3A), the increase was 2-fold. A blue shift of 43 nm for 2-*m*DMAT and 2 nm for 7-*m*DMAT and 10-*m*DMAT accompanied this change. The results suggest that all three analogues bind rapidly to tubulin. These experiments were done at room temperature in the absence of GTP, conditions under which the analogue-induced assembly would have been very slow, especially at the low tubulin concentration used. To examine changes under polymerization conditions, the reactions were carried out at 37 °C in the presence of 10 μM tubulin, 0.5 mM GTP, and 10 μM analogue. In the case of 2-*m*DMAT (Figure 2B), an immediate increase of fluorescence again occurred followed by a time-dependent increase. The fluorescence increase during the time-dependent process was about 7-fold higher than that obtained under nonassembly conditions, consistent with the increase being due to tubulin assembly and a higher affinity of paclitaxel and its analogues for the polymerized form of tubulin (the fluorescence intensities in panels A and B of Figure 2 are in arbitrary units and cannot be compared directly). The increase also correlated well with the increase in light scattering at 350 nm, reflecting the polymerization reaction (Figure 2C). When 10 μM paclitaxel was also present, the increase in fluorescence associated with microtubule formation was prevented (Figure 2B) even though the increase in light scattering in the presence of 10 μM paclitaxel was 3-fold higher than that with 10 μM 2-*m*DMAT alone (Figure 2C). These data are similar to those presented previously for N-*m*DMAT (Sengupta et al., 1995).

A completely different picture was obtained with 7-*m*DMAT and 10-*m*DMAT under assembly conditions. After the instantaneous increase in drug fluorescence, a time-dependent quenching of fluorescence was observed. The data for the 10-derivative are presented in Figure 3B. The final fluorescence was about 50% of the value obtained for the same concentration of the free drug. Under the same conditions, there was a time-dependent increase in light scattering at 350 nm, which was coincident with the quenching process. When 10 μM paclitaxel was included

Table 2: Effect of Solvents on the Emission Maxima of the Paclitaxel Analogues

solvent	dielectric constant[a]	N-*m*DMAT	N-*p*DMAT	2-*m*DMAT	7-*m*DMAT	10-*m*DMAT	3′-*m*DMAT
water	78.5	469	378	488	452	460	370
acetonitrile	39.0	441	362	467	445	460	355
methanol	32.6	455	363	473	465	472	357
2-propanol	18.3	437	362	462	451	462	352
cyclohexane	2.02	405	335	430	432	437	327
3% ethanol in cyclohexane		443		450	450	460	
tubulin		445		445	450	458	

[a] The dielectric constants are at 25 °C.

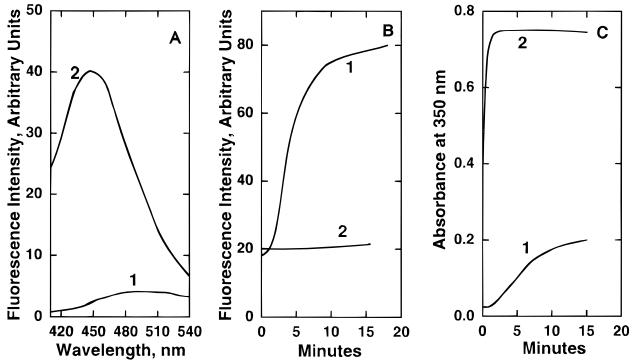

FIGURE 2: Binding of 2-*m*DMAT to tubulin and microtubules. (A) 2-*m*DMAT (5 μM) and 5 μM tubulin at 25 °C in PEM buffer. The fluorescence emission spectrum was recorded using 350 nm as the excitation wavelength: 2-*m*DMAT (curve 1) and 2-*m*DMAT with tubulin (curve 2). (B) Time course of fluorescence intensity change at 450 nm under polymerizing conditions. Tubulin (10 μM) in PEM buffer containing 0.5 mM GTP and 10 μM 2-*m*DMAT (curve 1) or 10 μM 2-*m*DMAT and 10 μM paclitaxel (curve 2) was incubated at 37 °C, and fluorescence intensity changes were recorded. (C) Time course of light scattering changes at 350 nm. Conditions were identical to those of part B, with 10 μM 2-*m*DMAT alone (curve 1) and both 10 μM 2-*m*DMAT and 10 μM paclitaxel (curve 2).

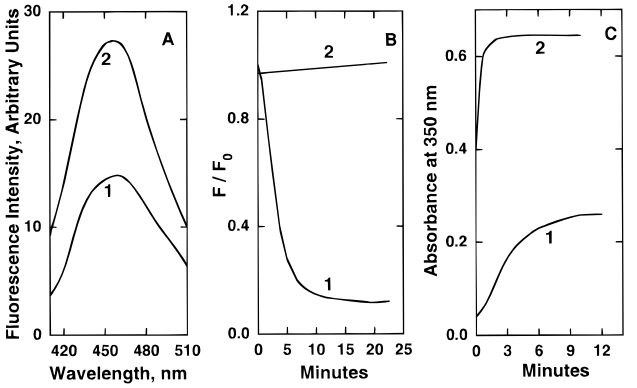

FIGURE 3: Binding of 10-*m*DMAT to tubulin and microtubules. The conditions are identical to those described in Figure 2. (A) 10-*m*DMAT (curve 1) and 10-*m*DMAT with tubulin (curve 2). (B) Time course of fluorescence intensity changes during assembly. The fluorescence values were normalized by dividing by the initial fluorecence value: 10-*m*DMAT (curve 1) and both 10-*m*DMAT and paclitaxel (curve 2). (C) Time course of light scattering changes during assembly. 10-*m*DMAT alone (curve 1) and both 10-*m*DMAT and paclitaxel (curve 2).

in the reaction mixture, quenching did not occur, even though the increase in light scattering took place (Figure 3C).

Binding of the Paclitaxel Analogues to Dimeric Tubulin. The instantaneous changes in fluorescence shown in Figures 2A and 3A indicate that the fluorescent analogues bind to the tubulin dimer. To test this more thoroughly, binding was studied in the presence of podophyllotoxin, a drug which prevents microtubule formation. An instantaneous increase in fluorescence was observed with all the analogues. A representative figure with 2-*m*DMAT is shown in Figure 4. Paclitaxel (30 μM) did not affect this increase (data not shown). When observed with an electron microscope, no trace of microtubule formation was found, even after incubating the reaction mixture for 60 min. These results are quite similar to what had been previously observed for N-*m*DMAT (Sengupta et al., 1995) and indicate that these derivatives also bind to dimeric tubulin.

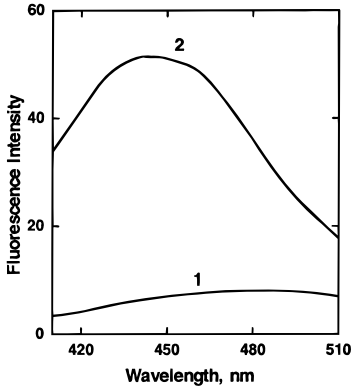

FIGURE 4: Binding of 2-*m*DMAT to the tubulin−podophyllotoxin complex. The fluorescence spectrum of 5 μM 2-*m*DMAT (curve 1) in PEM buffer at 25 °C was compared to its spectrum in the presence of 5 μM tubulin−podophyllotoxin (curve 2). The tubulin−podophyllotoxin complex was prepared by incubating 5 μM tubulin with 40 μM podophyllotoxin for 30 min at 25 °C.

DISCUSSION

In an effort to obtain insight into the mechanism of paclitaxel binding to tubulin and the nature of the environment around different parts of the paclitaxel molecule in the bound state, we have synthesized fluorescent paclitaxel analogues with the fluorescent group at the 2-, 3′-, 7-, 10-, and *N*-positions. Previous studies have shown that the *N*-benzoyl, 2-benzoyl, 3′-phenyl, 7-OH, and the 10-acetyl groups of paclitaxel can tolerate a number of substitutions without causing large changes in the activity of the drug (Hepperle & Georg, 1994; Georg et al., 1995b,c). However, modifications of the 7-hydroxy group with bulky substituents can decrease activity significantly (Georg et al., 1992; Riomoldi et al., 1993). Our results with the dimethylamino derivatives, showing a larger decrease in tubulin assembly-promoting activity for 7-*m*DMAT compared to those of the other analogues (Table 1), are consistent with the past results.

The effect of solvents on the fluorescence spectra of the derivatives indicates that the fluorophoric groups of all the analogues form hydrogen bonds in protic solvents. This study also showed that 7-*m*DMAT and 10-*m*DMAT behave differently compared to the other analogues in the presence of water, as their emission maxima are more blue-shifted in

water than in methanol, reflecting a difference in the environment around the fluorophore. The fluorophore in 7-*m*DMAT is close to the 9-carbonyl and 10-acetyl carbonyl groups. In 10-*m*DMAT, it is close to the 9-carbonyl and 7-OH. A possible explanation for the behavior of these derivatives in water is that water hydrates one or more of the carbonyl groups, increasing the cavity radius in which the fluorophore resides. This in turn decreases the Stokes shift (the difference between the absorption and emission maxima) according to the Lippert equation (Lippert, 1957), by causing a decrease in the emissiom maxima. As a result, these two derivatives have lower emission maxima in water than would be expected.

Binding of the four analogues to tubulin results in a blue shift in the emission maxima along with an increase in fluorescence intensity. However, the extent of the blue shifts differs among the analogues. The much smaller shifts of 7-*m*DMAT and 10-*m*DMAT, compared to those of 2-*m*DMAT and N-*m*DMAT (Sengupta et al., 1995), suggest that the 7- and 10-positions are in a less hydrophobic environment than the 2- and *N*-positions. This conclusion is supported by the data in Table 2 that show the maxima of the bound forms of the 7- and 10-derivatives to be close to that found in water, whereas the maxima for the 2- and *N*-derivatives have values more consistent with a nonpolar solvent having a dielectric constant close to that of acetonitrile. However, the emission maxima of the 2- and *N*-analogues in cyclohexane containing 3% ethanol are also very close to that of the tubulin-bound form, indicating that these positions of paclitaxel might be situated in a more hydrophobic region of the protein than is reflected by the relationship between the dielectric constants and emission maxima but are accessible to groups with which they can hydrogen bond. Both the nitrogen and carbonyl functions of the benzoyl group could then participate in hydrogen bonding. The possibility that the carbonyl of the C2 benzoyl group may participate in hydrogen bonding in tubulin has been suggested previously (Mastropaolo et al., 1995). In cyclohexane/3% ethanol, 7-*m*DMAT and 10-*m*DMAT have emission maxima similar to that in water and in the tubulin-bound form, suggesting that the 7- and 10-positions are in a relatively hydrophilic environment.

Another major difference between the analogues is the fluorescence changes upon binding to microtubules. In the case of N-*m*DMAT and 2-*m*DMAT, binding led to a large increase in fluorescence intensity. In contrast, binding of 7-*m*DMAT and 10-*m*DMAT to polymeric tubulin led to a dramatic quenching. A possible explanation for the quenching is that the fluorophoric groups undergo π stacking with aromatic amino acids of the protein. A similar quenching has been shown for the interaction of anthracyclins with serum albumin (Rivory et al., 1992) or with DNA (Chaires et al., 1982) and for the myosin subfragment-1 interaction with pyrene-labeled actin (Blanchoin et al., 1996). Another possible reason for the quenching is that the fluorophoric groups are close to charged side chains of the protein (Demchenko, 1992). For example, quenching of Trp314 of liver alcohol dehydrogenase at alkaline pH has been attributed to the ionization of Tyr286 (Eftink & Bystrom, 1986). It must be remembered that, in the case of the 7- and 10-derivatives, benzoyl groups have been added to the paclitaxel molecule, whereas these rings already exist in the 2- and *N*-derivatives. Thus, the addition of these groups to the 7- and 10-positions of paclitaxel may place them in an environment that, in the polymeric state, comes in close contact with aromatic amino acids or charged residues.

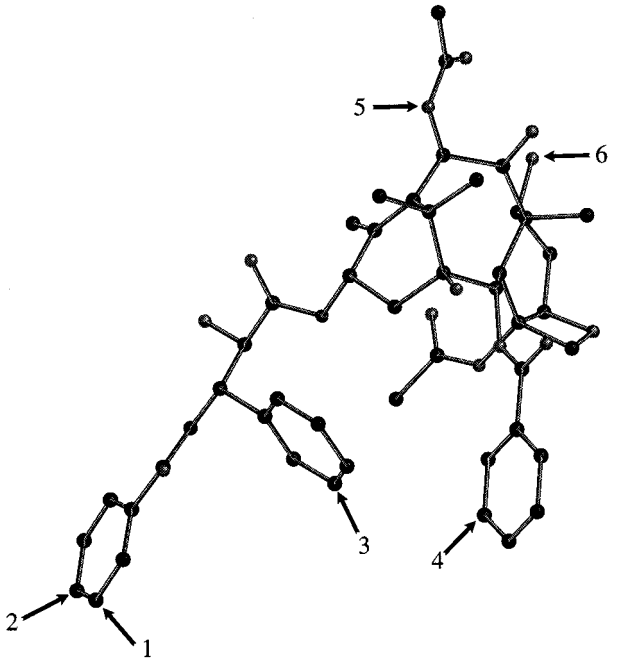

FIGURE 5: Three-dimensional structure of paclitaxel. The positions of the substitutions for the six fluorescent analogues are shown by arrows: 1, N-*m*DMAT; 2, N-*p*DMAT; 3, 3′-*m*DMAT; 4, 2-*m*DMAT; 5, 10-*m*DMAT; and 6, 7-*m*DMAT.

The observations described above indicate a binding model in which the 2- and *N*-benzoyl groups bind in a hydrophobic pocket of tubulin and the region of paclitaxel containing the 7- and 10-positions is in a more hydrophilic environment. That the environments of the *N*- and 2-benzoyl, as well as the 3′-phenyl and 4-acetyl groups, can be different from that of the 7-hydroxy and 10-acetyl groups is evident from NMR studies of paclitaxel and water-soluble paclitaxel derivatives (Vander Velde et al., 1993; Williams et al., 1993, 1994; Paloma et al., 1994), and the crystal structure of paclitaxel (Mastropaolo et al., 1995). It is also clear from the computer-generated three-dimensional structure of paclitaxel (Figure 5) that the 7- and 10-functions occupy positions far from the 2- and *N*-functions. Modeling of the six derivatives in Figure 5 showed that the structures did not deviate from the paclitaxel structure.

Similar to our earlier findings with N-*m*DMAT (Sengupta et al., 1995), we found evidence for binding of the 2-, 7-, and 10-analogues to dimeric tubulin and to the tubulin−podophyllotoxin complex. In the previous work, we found that N-*m*DMAT binds weakly to tubulin−podophyllotoxin with a K_d of 49 μM. This is in contrast to the K_d for the binding of paclitaxel to polymeric tubulin which is reported to be 10 nM (Caplow et al., 1994) and explains why paclitaxel, assuming its affinity is also so weak, cannot prevent binding of the analogue since under the conditions used, 30 μM paclitaxel and 5 μM analogue, only 40% of the binding sites would be occupied. Binding to the tubulin−podophyllotoxin complex receives support from the work of Han et al. (1996), who demonstrated binding of the 2-aminobenzoyl derivative of paclitaxel to the tubulin−colchicine complex, and Carlier and Pantaloni (1983), who showed that paclitaxel stimulates the GTPase activity of the tubulin−colchicine complex. On the other hand, Han et al.

(1996) concluded that the fluorescence increase of the 2-aminobenzoyl analogue in the presence of tubulin but without colchicine was due to the formation of microtubules. However, with N-*m*DMAT, this increase is observed in the presence of concentrations of urea (Sengupta et al., 1996) that are known to inhibit microtubule formation but not cause tubulin unfolding (Sackett et al., 1994). Moreover, the fluorescence of 7-*m*DMAT and 10-*m*DMAT was quenched when bound to microtubules but enhanced when these compounds were added to tubulin under nonassembly conditions. Thus, the enhancement observed in these cases could not be due to the formation of microtubules. It is not possible to say whether the site in the dimer to which paclitaxel and the fluorescent derivatives bind is the same site that exists in polymerized tubulin. If it is, the environment around the 7- and 10-positions must undergo a change upon polymerization, to account for the change in fluorescence from enhancement to quenching. Such a change could result from the interaction with a neighboring dimer in the microtubule, a process that could also cause the large increase in binding affinity.

ACKNOWLEDGMENT

We thank Dr. Sam F. Victory for performing the molecular modeling structure determinations.

SUPPORTING INFORMATION AVAILABLE

Detailed syntheses of all of the analogues and intermediates and NMR assignments (10 pages). Ordering information is given on any current masthead page.

REFERENCES

Algaier, J., & Himes, R. H. (1988) *Biochim. Biophys. Acta 954*, 235−243.

Blanchoin, L., Didry, D., Carlier, M. F., & Pantaloni, D. (1996) *J. Biol. Chem. 271*, 12380−12386.

Bollag, D. M., McQueney, P. A., Zhu, J., Hensens, O., Koupal, L., Liesch, J., Goetz, M., Lazarides, E., & Woods, C. M. (1995) *Cancer Res. 55*, 2325−2333.

Bradford, M. M. (1976) *Anal. Biochem. 72*, 248−256.

Caplow, M., Shanks, J., & Ruhen, R. (1994) *J. Biol. Chem. 269*, 23399−23402.

Carlier, M.-F., & Pantaloni, D. (1983) *Biochemistry 22*, 4814−4822.

Chaires, J. B., Dattagupta, N., & Crothers, D. M. (1982) *Biochemistry 21*, 3933−3940.

Datta, A., Hepperle, M., & Georg, G. I. (1995) *J. Org. Chem. 60*, 761−763.

Demchenko, A. P. (1990) in *Topics in Fluorescence Spectroscopy* (Lakowicz, J. R., Ed.) Vol. 3, pp 65−111, Plenum Press, New York.

Derry, W. B., Wilson, L., & Jordan, M. A. (1995) *Biochemistry 34*, 2203−2211.

Eftink, M. R., & Bystrom, K. (1986) *Biochemistry 25*, 6624−6630.

Georg, G. I., Harriman, G. C. B., Himes, R. H., & Mejillano, M. (1992) *Bioorg. Med. Chem. Lett. 2*, 735−738.

Georg, G. I., Boge, T. C., Cheruvallath, Z. S., Harriman, G. C. B., Hepperle, M., Park, H., & Himes, R. H. (1994) *Bioorg. Med. Chem. Lett. 4*, 335−338.

Georg, G. I., Ali, S. M., Boge, T. C., Datta, A., Falborg, L., Park, H., Mejillano, M., & Himes, R. H. (1995a) *Bioorg. Med. Chem. Lett. 5*, 259−264.

Georg, G. I., Boge, T. C., Cheruvallath, Z. S., Clowers, J. S., Harriman, G. C. B., Hepperle, M., & Park, H. (1995b) in *Taxol Science and Applications* (Suffness, M., Ed.) pp 317−375, CRC, Boca Raton, FL.

Georg, G. I., Harriman, G. C. B., Vander Velde, D. G., Boge, T. C., Cheruvallath, Z. S., Datta, A., Hepperle, M., Park, H., Himes, R. H., & Jayasinghe, L. (1995c) in *Taxane Anticancer Agents: Basic Science and Current Status* (Georg, G. I., Chen, T. T., Ojima, I., & Vyas, D. M., Eds.) ACS Symposium Series 583, pp 217−232, American Chemical Society, Washington, DC.

Georg, G. I., Harriman, G. C. B., Hepperle, M., Clowers, J. S., Vander Velde, D. G., & Himes, R. H. (1996a) *J. Org. Chem. 61*, 2664−2676.

Georg, G. I., Liu, Y., Boge, T. C., & Himes, R. H. (1996b) *Bioorg. Med. Chem. Lett.* (in press).

Han, Y., Chaudhary, A. G., Chordia, M. D., Sackett, D. L., Perez-Ramirez, B., Kingston, D. G. I., & Bane, S. (1996) *Biochemistry 35*, 14173−14183.

Hepperle, M., & Georg, G. I. (1994) *Drugs Future 19*, 573−584.

Jordan, M. A., Toso, R. J., Thrower, D., & Wilson, L. (1993) *Proc. Natl. Acad. Sci. U.S.A. 90*, 9552−9556.

Jordan, M. A., Wendell, K., Gardiner, S., Derry, W. B., Copp, H., & Wilson, L. (1996) *Cancer Res. 56*, 816−825.

Lippert, V. E. (1957) *Z. Electrochem. 61*, 962−975.

Mastropaolo, D., Camerman, A., Luo, Y., Brayer, G. D., & Camerman, N. (1995) *Proc. Natl. Acad. Sci. U.S.A. 92*, 6920−6924.

Paloma, L. G., Guy, R. K., Wrasidlo, W., & Nicolaou, K. C. (1994) *Chem. Biol. 1*, 107−112.

Rao, K. V., Bhakuni, R. S., Johnson, J., & Oruganti, R. S. (1995) *J. Med. Chem. 38*, 3411−3414.

Riomoldi, J. M., Kingston, D. G. I., Chaudhary, A. G., & Samaranayake, G. (1993) *J. Nat. Prod. 56*, 1313−1330.

Rivory, L. P., Pond, S. M., & Winzor, D. J. (1992) *Biochem. Pharmacol. 44*, 2347−2355.

Schiff, P. B., & Horwitz, S. B. (1980) *Proc. Natl. Acad. Sci. U.S.A. 77*, 1561−1565.

Sengupta, S., Boge, T. C., Georg, G. I., & Himes, R. H. (1995) *Biochemistry 34*, 11889−11894.

Souto, A. A., Acuña, U., Andreu, J. M., Barasoain, I., Abal, M., & Amat-Guerri, F. (1995) *Angew. Chem., Int. Ed. Engl. 34*, 2710−2712.

ter Haar, E., Kowalski, R. J., Hamel, E., Lin, C. H., Longley, R. E., Gunasekera, S. P., Rosenkranz, H. S., & Day, B. W. (1996) *Biochemistry 35*, 243−250.

Tiwari, S. C., & Suprenant, K. A. (1993) *Anal. Biochem. 251*, 96−103.

Vander Velde, D. G., Georg, G. I., Grunewald, G. L., Gunn, C. W., & Mitscher, L. A. (1993) *J. Am. Chem. Soc. 115*, 11650−11651.

Williams, H. J., Scott, A. I., & Dieden, R. A. (1993) *Tetrahedron 49*, 6545−6560.

Williams, H. J., Scott, A. I., & Dieden, R. A. (1994) *Can. J. Chem. 72*, 252−260.

Yvon, A. C., Wendell, K., Wilson, L., Jordan, M. A., & Wadsworth, P. (1996) *Mol. Biol. Cell 7* (Suppl.), 576a.

Zheng, Q. Y., Darbie, L. G., Cheng, X., & Murray, C. K. (1995) *Tetrahedron Lett. 36*, 2001−2004.

BI962891M